ISSN 0001-4338, Izvestiya, Atmospheric and Oceanic Physics, 2006, Vol. 42, No. 3, pp. 337–352. © Pleiades Publishing, Inc., 2006.
Original Russian Text © G.N. Panin, A.E. Nasonov, T. Foken, 2006, published in Izvestiya AN. Fizika Atmosfery i Okeana, 2006, Vol. 42, No. 3, pp. 367–383.

Evaporation and Heat Exchange of a Body of Water with the Atmosphere in a Shallow Zone

G. N. Panin[a], A. E. Nasonov[a], and T. Foken[b]

[a] *Water Problems Institute, Russian Academy of Sciences, ul. Gubkina 3, Moscow, 119991 Russia*
e-mail: panin@aqua.laser.ru
[b] *Micrometeorology Department, University of Bayreuth, D-95440 Bayreuth, Germany*

Received March 1, 2005; in final form, November 10, 2005

Abstract—Results are reported from experimental and theoretical studies of the energy and mass exchange of a body of water with the atmosphere. A new parametric model has been developed on the basis of experimental data that takes into account the influence of the depth of the basin on evaporation, its heat exchange with the atmosphere, and the water-surface friction at different wind speeds. Comparison of the model with measurements during the LITFASS-98 and LITFASS-2003 experiments (Germany) shows good consistency. The results indicate, on the one hand, that the depth of the basin has a large effect on the intensity of energy exchange under natural conditions. On the other hand, the examples shown in the paper illustrate good agreement of the model calculations with experimental data. On the basis of the experimental data on the influence of the basin depth on the intensity of the interaction between the basin and the atmosphere, a balance model of the energy exchange in the coastal zone has been developed. The balance model calculates the momentum, heat, and moisture fluxes at different distances from the shore. Results of using the new model to estimate the intensification of evaporation and the heat exchange of the northern Caspian and the Kara-Bogaz Gol are discussed.

DOI: 10.1134/S0001433806030078

1. INTRODUCTION

Evaporation and heat exchange are the main components of the water and heat balance of a basin. For this reason, their determination has been historically of special interest. The rate of evaporation and heat exchange depends on the properties of air masses moving over the sea and is determined mainly by conditions of the underlying sea surface. A fairly reliable method for measuring evaporation and heat exchange is a straightforward method based on direct measurements of turbulent fluctuations of air humidity and temperature and the vertical wind component with a further calculation of the instantaneous vertical fluxes [1]. The time averaging of these quantities gives flux values at a point. To determine the evaporation and heat exchange for a certain water area, their values need to be measured at many sites, a procedure that is not as yet possible. Therefore, this problem is solved by parametrization of turbulent fluxes [2, 3], with a further derivation of empirical relationships.

To determine the evaporated water and heat exchange, various methods are used, among which two basic classes are noteworthy: (1) methods using the equations of the water and heat balance of the sea and (2) methods using empirical and semiempirical relationships of different kind.

The balance methods are known to give an integral value of visible evaporation from the entire basin and the heat exchange of the basin. Often, it is the integral quantity that is required to carry out water-management calculations, so the balance methods are most widespread in practice. At the same time, it should be kept in mind that the capability of the balance methods for determining local evaporation and heat exchange are limited by the assumption of spatial homogeneity of these characteristics, which is not fulfilled in most cases.

Apart from this major shortcoming of the balance method, it is clear that the evaporation and heat exchange can be determined indirectly, as a closure term in the water and heat balance equation. In this case, the errors in the terms of the equation will become the errors of the sought variables.

The methods of the second type for the indicated range have an important advantage: they calculate values of the true, not visible, evaporation. In addition, the methods of the second type give insight into the spatial variability of evaporation and heat exchange and allow one to examine their regional features. Finally, integration of evaporation and heat exchange with respect to area should give information about the resultant (integral) evaporation and heat exchange. A disadvantage of this method is the use of simple semiempirical relations in which the complex nature of the air–sea interaction is disregarded for the calculation of evaporation and heat exchange. In particular, the estimates of the magnitudes of evaporation and heat exchange are still made with no correction for

basin depth. It is evident, however, that the shallow basins must evaporate faster than the deep ones.

Previous investigations [4] have shown that changes in the water-balance components account for only 90% of the current sea-level variations of the Caspian Sea. There may be a number of factors that induce the indicated imbalance, but we supposed that it could have been caused by an insufficiently correct calculation of the evaporation from the shallow northern Caspian. An overview of the methods of calculation of evaporation and the heat and energy exchange has demonstrated that the state-of-the-art models of the heat and mass exchange between a basin and the atmosphere do not take into account the small-scale interaction between the shallows and the atmosphere. The point is that waves in shallow water are steeper than in the open and deep-water parts of the sea and break earlier (at lower wind speeds). These peculiarities must lead to an increase in the aerodynamic roughness of the water surface and, consequently, to a more intense turbulent exchange of momentum, heat, and moisture. It is possibly owing to these conditions that the Kara-Bogaz Gol, after it became isolated from the Caspian in 1980, was drying up almost twice as rapidly than expected. The overview has also shown that a reliable method of estimation of the evaporation and heat exchange of shallow lakes and coastal areas does not exist so far. This situation has initiated a new field in the investigations at the Land Water–Atmosphere Interaction Laboratory of the Water Problems Institute, Russian Academy of Sciences, with emphasis on the development of theories about the nature of the interaction between a shallow basin and the atmosphere. Investigations have been carried out both experimentally and theoretically.

2. ANALYSIS OF MEASUREMENTS OF THE SURFACE FLUXES OF MOMENTUM, HEAT, AND MOISTURE IN THE SHALLOW NORTHERN CASPIAN

The main experimental data were obtained at the shallow northern Caspian. Three expeditions were conducted on the R/V *Akvatoriya* from 1990 through 1992. The main objectives of the experiment were to measure turbulent momentum, heat, and moisture fluxes; surface waves; and related hydrometeorological parameters at different depths of the sea.

The equipment for measurements of heat, moisture, and momentum fluxes and instruments for measurement of surface waves and accompanying hydrometeorological data were installed on the tower of and aboard the R/V *Akvatoriya* at different sites of the northern Caspian and at different depths (from 3 to 8 m). The signal from the instruments was transmitted over a cable to the R/V *Akvatoriya*, where it was recorded on a computer and preprocessed. The vessel was anchored at a distance of 20 to 25 m from the tower. This setup allowed obtainment of data on surface fluxes and accompanying information under relatively undisturbed conditions. The equipment passed appropriate tests during the KUREX-99 [5] and FIFE-89 [6] international experiments.

The unique information thus obtained was further used for direct analysis of the intensity of evaporation and heat and momentum exchange depending on the depth of the sea and wind-wave parameters. Hydrometeorological information was used to calculate surface fluxes of momentum, heat, and moisture by using the bulk parametrizations for a deep sea [3, 7–10].

Our first experimental data have already shown significantly larger values of the interaction characteristics in comparison with their typical values under similar hydrometeorological conditions in deep water. This is illustrated by the relationship between the drag coefficient C_D and the parameters C_0/U_* (where C_0 is the phase velocity of the major harmonic of surface waves and U_* is the above-water wind friction velocity) and h/H (where h is the height of surface waves and H is the depth of the sea at a measurement point), which characterize the dynamic state of surface waves (Figs. 1a, 1b). The drag coefficient C_D changes by about an order of magnitude from values of less than 1×10^{-3} to 6×10^{-3}. With moderate wind waves ($C_0/U_* > 20$; $h/H < 0.1$), the experimental points concentrate around $C_D \approx 1 \times 10^{-3}$, a typical value for deep water. As the wind becomes stronger, surface waves in shallow water begin to break earlier than in deep water. As a result, the friction of the water surface increases sharply even with a small increase in the parameters C_0/U_* and h/H and the drag coefficient C_D attains 6×10^{-3} when $C_0/U_* \approx 10$ and $h/H \approx 0.15$, respectively.

The effect of the enhancement of the water-surface friction and of the intensity of evaporation and heat exchange between shallow water and the atmosphere as compared to deep water is most clearly seen in Fig. 2a. Comparison of the measured drag coefficients and Stanton (C_T) and Dalton (C_e) numbers with those calculated by bulk parametrizations (Panin, 1985) under different dynamic states of surface waves (h/H) shows that the measured values are more than twice as large as those calculated for deep water.

The difference between the measured heat and moisture fluxes on the one hand and their bulk parametrizations [2, 3, 10] on the other attains 500 W/m^2 in different dynamic states of surface waves (C_0/U_* and h/H) (Figs. 2b, 2c). At the same time, during moderate wind waves ($C_0/U_* > 20$; $h/H < 0.1$), it is seen in Figs. 2b and 2c that the model calculations agree well with the measured moisture and heat fluxes. When h/H is less than 0.1 ($h/H < 0.1$), the waves are low and result in no

additional intensification of the vertical exchange processes.

It is evident that, during moderate wind waves in shallow areas, the breaking of waves is still not observed. In this case, we obtain the expected result: the calculated data are consistent with measurements (the discrepancies generally do not exceed 100 W/m^2, and they are random). Figures 2b and 2c, therefore, clearly illustrate a satisfactory simulation of the results by the model computations (formulas (4) and (5)) when $h/H < 0.1$.

3. THEORETICAL GENERALIZATIONS AND PARAMETRIZATION OF HEAT EXCHANGE AND EVAPORATION IN THE BOUNDARY LAYER ABOVE A BASIN

By means of spectral analysis of wind, temperature, and humidity on the one hand and of surface waves in a deep basin on the other, it was shown [3, 10–14] that temperature and moisture spectra, as well as cospectra of heat and moisture fluxes, are far less subject to the wave effect than the spectra of wind velocity and cospectra of momentum fluxes. This means that self-similarity conditions can be more widely used in describing evaporation and heat exchange of a basin with the atmosphere than in describing the characteristics of dynamic interaction.

In this case, the change in the heat exchange and evaporation in the boundary layer over a basin is easier to describe as

$$C_{T,e} = F_{T,e}(z/h_S;\ z/L;\ h_S/\delta_\nu;\ \mathrm{Pr}_T;\ \mathrm{Pr}_e). \quad (1)$$

With the Prandtl numbers held constant and equal to one another ($\mathrm{Pr}_T = \mathrm{Pr}_e = \mathrm{Pr} = 1.0$) and the measurement height being fixed (for example, $z = 10$ m), formula (1) can be rewritten as

$$C_{T,e} = F_{T,e}(z/L;\ h_S/\delta_\nu). \quad (2)$$

Assuming that δ_ν in (2) can be represented to within a numerical factor as $\delta_\nu \sim \nu/u_*$ and $h_s \sim z_0$, we have

$$C_{T,e} = F_{T,e}(z/L;\ z_0u_*/\nu). \quad (3)$$

The determination of the form of $F_{T,e}$ is discussed in many publication [10, 15, 16]. We consider the final formulas that formed the basis for the calculation of evaporation and heat exchange of a deep sea

$$E = C^N_{T,e}\rho U_Z \Delta q_{SZ}\begin{cases} A\rho c_P \Delta q_{SZ}^{4/3}\left[\dfrac{\beta\nu_E^2 g}{\nu}(1 + b/\mathrm{Bo})\right]^{1/3} & \text{at } U_{10} < 3 \text{ m/s} \\ (1 - z/L)[1 + 10^{-2}(z_0u_*/\nu)^{3/4}] & \text{at } z/L < 0 \\ [1/(1 + 3.5z/L)][1 + 10^{-2}(z_0u_*/\nu)^{3/4}] & \text{at } z/L > 0, \end{cases} \quad (4)$$

$$H_T = C^N_{T,e}\rho c_P U_Z \Delta T_{SZ}\begin{cases} A\rho c_P \Delta T_{SZ}^{4/3}\left[\dfrac{\alpha\nu_T^2 g}{\nu}(1 + b/\mathrm{Bo})\right]^{1/3} & \text{at } U_{10} < 3 \text{ m/s} \\ (1 - z/L)[1 + 10^{-2}(z_0u_*/\nu)^{3/4}] & \text{at } z/L < 0 \\ [1/(1 + 3.5z/L)][1 + 10^{-2}(z_0u_*/\nu)^{3/4}] & \text{at } z/L > 0. \end{cases} \quad (5)$$

In (4) and (5), $\alpha = -(\partial\ln\rho/\partial T)_{p,q} = 1/T_Z$ is the coefficient of thermal expansion of air; $\beta = -(\partial\ln\rho/\partial q)_{p,T} \approx 0.61$; ν_T and ν_E are the kinematic coefficients of molecular diffusion of heat and water vapor in the air, respectively; $b = \beta c_P/\alpha\lambda \approx 0.073$ (at $T_Z = 297$ K); g is the gravitational acceleration; ρ is the air density; c_P is the specific heat of air at constant pressure; Bo is the Bowen ratio ($\mathrm{Bo} = H_T/\lambda E$); A is a coefficient (A = 0.15); and L is the Monin–Oboukhov length.

Finally, from standard hydrometeorological data T_S, T_z, q_z, U_z, and z, the values of evaporation and heat exchange of a deep sea with the atmosphere can be determined directly from (4) and (5).

Parametrization of Interaction of a Shallow Sea with the Atmosphere

Note that the sensitivity of evaporation and heat exchange to the depth of a basin was pointed out earlier (see [10, 12, 17, 16]). The intensification of the energy and mass exchange between a shallow basin and the atmosphere is caused by a change in the heat regime of the basin [18, 19] as well as by a change in the aerodynamic roughness of its surface [17, 20]. Whereas thermal changes are taken into account in the calculations through the use of actual data on surface temperature, the roughness changes are usually disregarded.

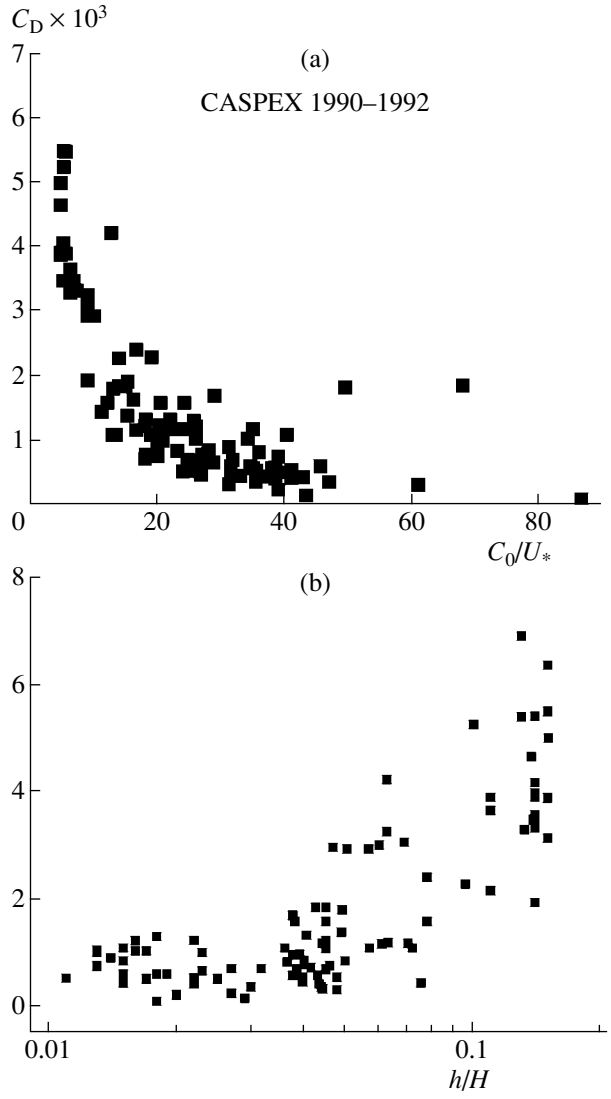

Fig. 1. Drag coefficient of water surface as a function of (a) dynamic state of surface waves (C_0/U_*) and (b) parameter h/H from the CASPEX experiment of 1990–1992.

The effect of increasing the aerodynamic surface roughness of shallows on the intensification of evaporation E and heat exchange H_T and on the behavior of the drag coefficient C_D and the coefficients of heat and mass exchange $C_{T,e}$ is shown in Figs. 2a–2c. Overall, these data allowed the intensity of evaporation, heat exchange, and energy exchange of shallows to be rep-

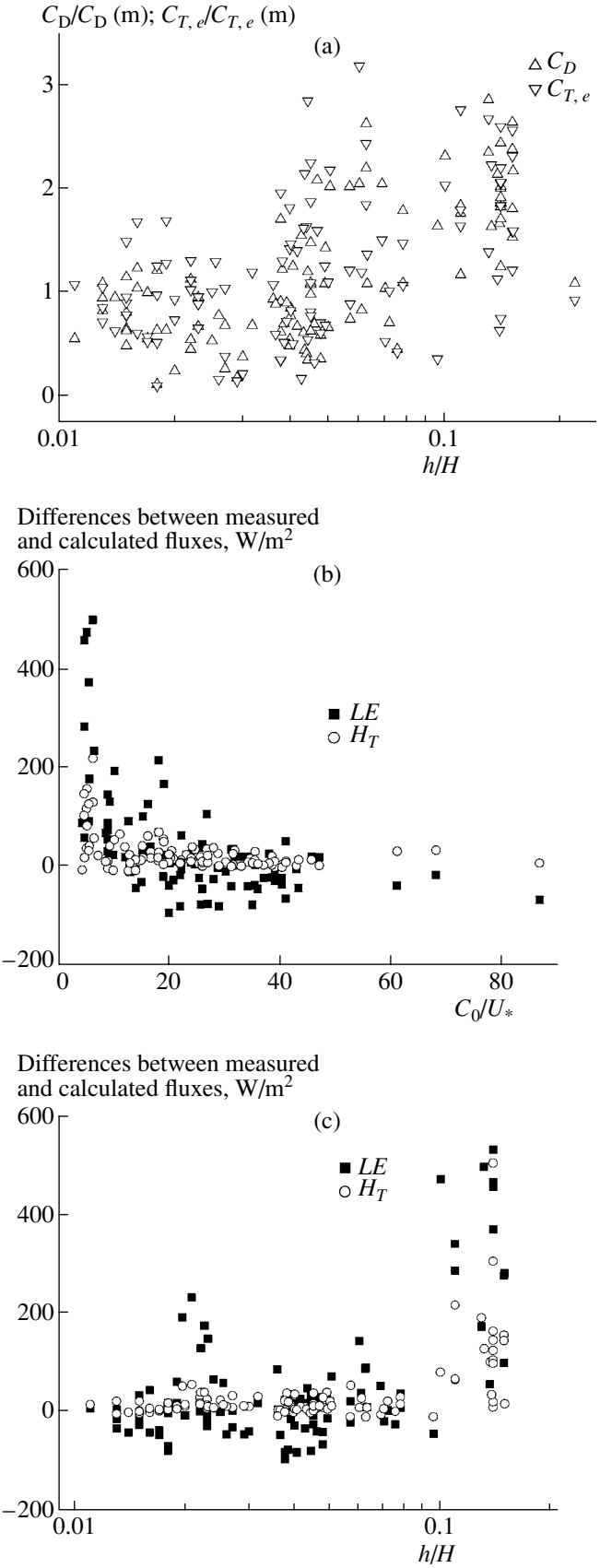

Fig. 2. (a) Ratios of the drag coefficient C_D and evaporation coefficient $C_{T,e}$ measured in shallow water to their calculated values C_D (m) and $C_{T,e}$ (m) from the deep-sea model (formulas (4) and (5)) as a function of the parameter h/H and the differences between the measured shallow-water latent (LE_M) and sensible (H_{TM}) heat fluxes and their calculated values from the deep-sea model (formulas (4) and (5)) as a function of (b) the dynamic state of surface waves (C_0/U_*) and (c) parameter h/H.

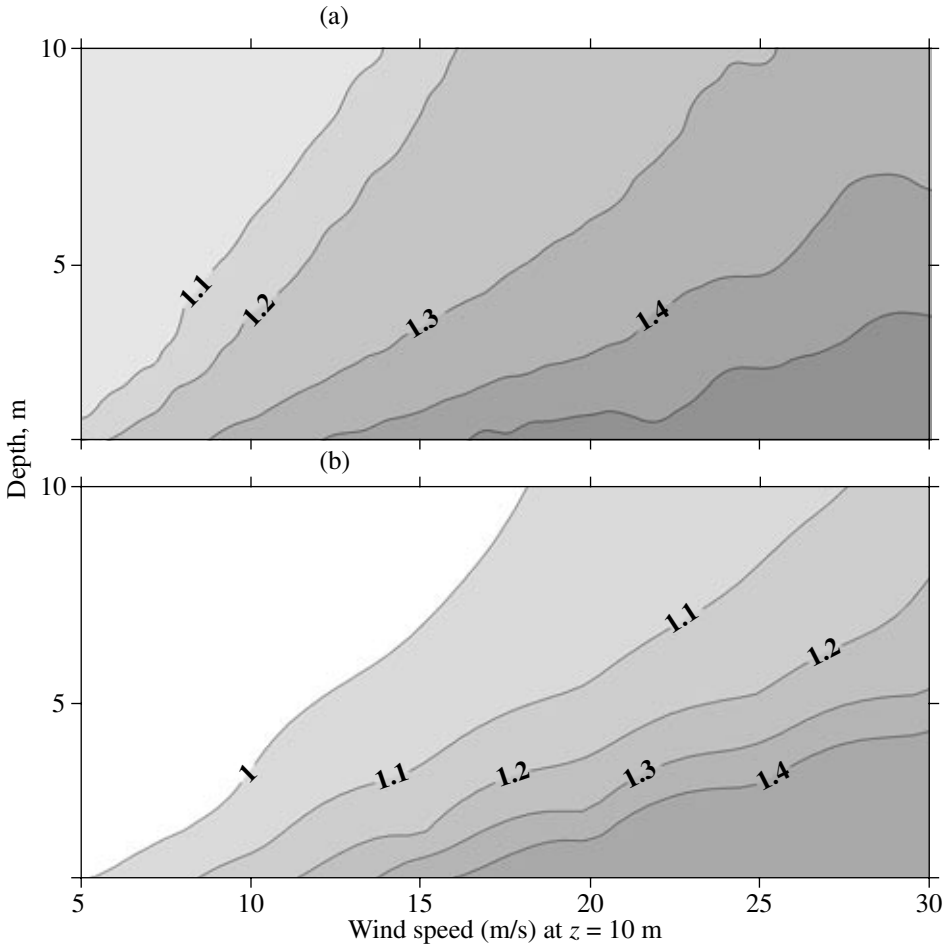

Fig. 3. (a) Coefficient of the intensification of evaporation and heat exchange between the water surface and the atmosphere and (b) wind friction velocity at different wind speeds at $z = 10$ m and different depths.

resented with an error of about 25% of the calculated value as

$$U_*^{\mathrm{SW}} = U_* + U_* k_U^{\mathrm{SW}} \frac{h}{H} \approx U_*(1 + 1.6h/H),$$

$$H_T^{\mathrm{SW}} = H_T + H_T k_T^{\mathrm{SW}} \frac{h}{H} \approx H_T(1 + 2h/H), \qquad (6)$$

$$E^{\mathrm{SW}} = E + E k_E^{\mathrm{SW}} \frac{h}{H} \approx E(1 + 2h/H),$$

where $k_T^{\mathrm{SW}} \approx k_E^{\mathrm{SW}} \approx 2.0$ and $k_U^{\mathrm{SW}} \approx 1.6$ are empirical coefficients.

In (6), h^{SW} is the shallow-water wave height to be measured.

Data on h^{SW} are often missing, so the empirical relation $h^{\mathrm{SW}} = \dfrac{0.07U_Z^2(gH/U_Z^2)^{3/5}}{g}$ can be used. The intensification of the energy and mass exchange between shallow basins and the atmosphere, obtained from empirical formulas (6), is illustrated in Figs. 3a and 3b for different wind speeds.

Effects of the Coastal Shallow Zone

It should be remembered that the air flow in the coastal zone is transformed [12, 16], which leads to additional difficulties in the calculation of the energy and mass exchange. A number of experimental and theoretical studies are available for this zone [21], including a comprehensive investigation of the structure of the internal boundary layer (IBL). However, quantitative estimates of the turbulent fluxes in this zone differ widely among investigators, while attaining 100% [20].

Using our own experimental data on the influence of the depth of a basin on the interaction intensity, we have developed a model of the energy and mass exchange in the coastal zone.

We use the notion of the surf zone ($x \le L^{(-)}$), where $h^{(-)}(x) = H^{(-)}(x)f(\tan\alpha) \approx 0.5H^{(-)}(x)$.

At the boundary of the coastal zone, it is possible to use dispersion relations for both a deep sea ($C_0 = g/\omega$) and a shallow sea ($C_0 = \sqrt{gH}$). As a result, we can write $\dfrac{\lambda^{(+)}}{H^{(+)}} = 2\pi \approx 6.28$.

The equation of the energy balance in the coastal zone for $\left(\dfrac{\lambda^{(+)}}{H^{(+)}} = 2\pi \approx 6.28\right)$ can be written as

$$\frac{\partial h^2}{\partial x} = \frac{h^{(+)2}}{L^{(+)}}\mathrm{F}(\tan\alpha). \tag{7}$$

The value of the function $\mathrm{F}(\tan\alpha)$ is found as

$$\int_{L^{(+)}}^{X} \frac{\partial h^2}{\partial x}dx = \frac{h^{(+)2}}{L^{(+)}}\int_{L^{(+)}}^{X} \mathrm{F}(\tan\alpha)dx. \tag{8}$$

After integration, we have

$$h^2(x) = h^{(+)2} - h^{(+)2}\frac{(L^{(+)} - x)}{L^{(+)}}\mathrm{F}(\tan\alpha). \tag{9}$$

For $x = L^{(-)}$, we obtain

$$h^{(-)} = 0.5H^{(-)} = 0.5\tan\alpha L^{(-)}. \tag{10}$$

Equation (9) is rewritten as

$$\begin{aligned} h^{(-)2} &= h^{(+)2} - h^{(+)2}\left(\frac{L^{(+)} - L^{(-)}}{L^{(+)}}\right)\mathrm{F}(\tan\alpha) \\ &= (0.5\tan\alpha)^2 L^{(-)2}. \end{aligned} \tag{11}$$

Let $\mathrm{F}(\tan\alpha) = c$. Then,

$$h^{(-)2} = h^{(+)2}\left[1 - c\left(1 - \frac{L^{(-)}}{L^{(+)}}\right)\right]. \tag{12}$$

$$\text{For } \frac{L^{(-)}}{L^{(+)}} \ll 1, \text{ we obtain } c \approx 1 - \left(\frac{h^{(-)}}{h^{(+)}}\right)^2. \tag{13}$$

It is clear from (12) and (13) that the parameter c depends on the type of coastal zone and its experimental determination is required for a particular basin. Assuming that $h^{(-)}/h^{(+)} = 0.5$, we obtain $c \approx 0.75$. Therefore, the final expression for the wave height in the coastal zone can be written as

$$\begin{aligned} h(x) &= h^{(+)}\left[1 - c\left(1 - \frac{x}{L^{(+)}}\right)\right]^{1/2} \\ &\approx h^{(+)}\left[0.25\left(1 - \frac{x}{L^{(+)}}\right)\right]^{1/2}, \end{aligned} \tag{14}$$

where x is the distance from the shore.

Using the mean statistical dependence of the wave height on wind velocity $h^{(+)} \approx 0.16\dfrac{U_Z^2}{g}$ [22] and the ratio $L^{(+)} = \dfrac{H^{(+)}}{\tan\alpha} = \dfrac{g}{\omega^2\tan\alpha} = \dfrac{\lambda^{(+)}}{2\pi\tan\alpha} \approx 2\dfrac{U_Z^2}{g\tan\alpha}$, we obtain the required expression for the wave height in the coastal zone in the final form

$$h(x) = 0.16\frac{U_Z^2}{g}\left[1 - c\left(1 - \frac{x}{2U_Z^2}g\tan\alpha\right)\right]^{1/2}. \tag{15}$$

Relation (15), when combined with empirical formulas (6), allows one to calculate heat, moisture, and momentum fluxes at different distances from the shore. For this purpose, it suffices to determine $\tan\alpha = \dfrac{H(x)}{L(x)} \approx \dfrac{H^{(+)}}{L^{(+)}}$ and the coefficient c.

First, we should make sure that our method of calculating the wave height in the coastal zone is correct. For this purpose, we used results of calculation of the wave height in the Baltic Sea [23] with the aid of the WAM model [24]. The wave parameters calculated with the WAM model were preliminarily compared with wave buoy measurements in the Baltic Sea. Comparison showed their good consistency. We now present the results of comparison (Fig. 4) of the wave heights from the Panin model with those obtained with the WAM model [24] at wind speeds varying from 2.5 to 20 m/s.

Calculations have shown that the models produce similar wave heights at wind speeds from 2.5 to 15 m/s and discrepancies appear at wind speeds above 15 m/s, attaining 0.5 m/s at a wind of 20 m/s.

For a quantitative estimation of heat, moisture, and momentum fluxes in the coastal zone of particular basins, information about these fluxes in the open, deep zone is required. This information can be obtained by conducting an experiment in a deep sea or

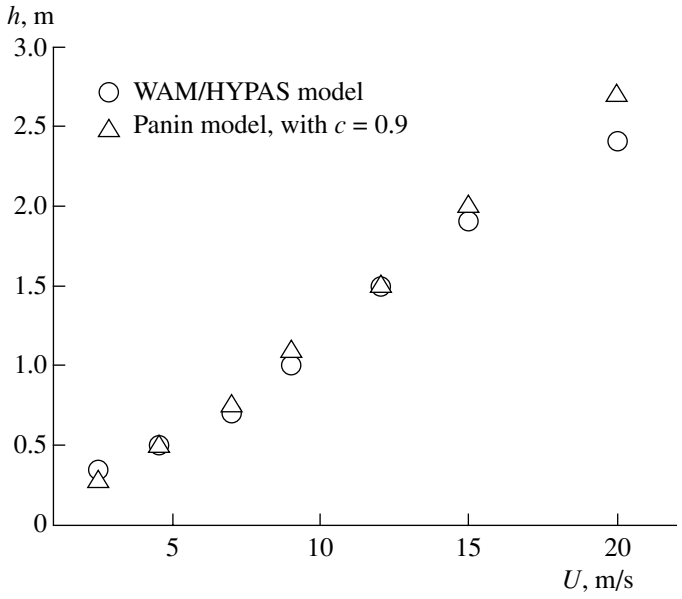

Fig. 4. Comparison of the calculated wave heights from the proposed model with those from the WAM model (WADIM Group, 1988) for wind speeds varying from 2.5 to 20 m/s.

by using the results from the model calculation (see formulas (4), (6)).

4. COMPARISON OF MODELED AND EXPERIMENTAL DATA

Shallow Basin

Data for testing the model of the heat and moisture exchange between shallow basins and the atmosphere were collected during the LITFASS-98 [25, 26] and LITFASS-2003 experiments. The experiments were conducted by efforts of scientists from leading German universities of Saxony (at the Meteorological Observatory Lindenberg, 50 km south of Berlin). During these experiments, surface fluxes were measured over different types of underlying surface, including Great Kossenblatt Lake (Fig. 5a). Vertical fluxes of heat, moisture, and momentum, along with radiation fluxes, were measured at a tower installed in the 2.5-m-deep lake (Fig. 5b).

The main results are presented in Figs. 6 and 7.

Figure 6 clearly illustrates the role of the shallow-water effect in the model computations of moisture fluxes. Comparison of the Panin model with the Foken model [7–9] for a deep sea has shown that the systematic discrepancy between the models is about 12% (Fig. 6a). The difference increases at large evaporation values and attains 75 W/m^2 when the evaporation is 300 W/m^2. The inclusion of the effect of evaporation intensification due to depth in the Foken model (Fig. 6b) leads to a nearly full coincidence of the model results (discrepancies being a mere 2%). Comparison of the model calculations with direct measurements of turbulent moisture fluxes (Fig. 7a) and total heat exchange ($LE + H_T$) also yielded reasonable results (Fig. 7b).

The error of simulation of the latent heat fluxes in the LIFTASS-2003 experiment by our model was 1%, with a correlation coefficient of 0.9. The total heat exchange ($LE + H_T$) is modeled with an error of 4%, the correlation coefficient being 0.9.

Coastal Shallow Zone

Very often, uncertainty arises in the choice of a relationship for the water-surface drag coefficient C_D. In most cases, the dependence of C_D on wind velocity is used in the form

$$10^3 C_D = a + bU_{10}. \quad (16)$$

Most often, (16) is used with the following values for the coefficients a and b [27]:

$$10^3 C_D = 0.75 + 0.067 U_{10}.$$

However, the majority of experiments were conducted in the coastal shallow zone, where surface waves, as was noted above, are steeper than in deep water. Therefore, the drag coefficient of water surface is to be increased and the interaction between shallows and the atmosphere is to be intensified. At the very least, it might be expected that the simple relation (16) should be corrected by taking into

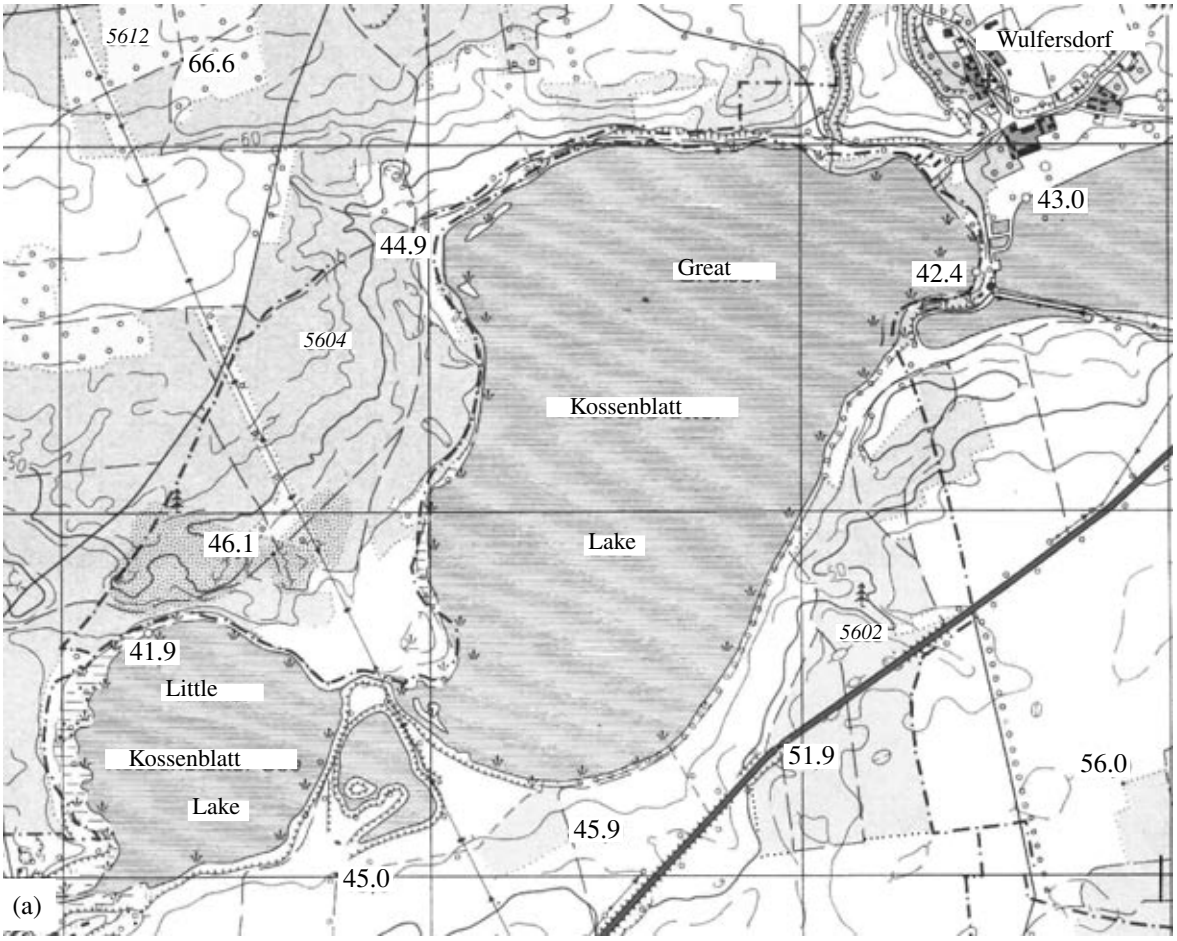

Fig. 5. (a) Great Kossenblatt Lake and (b) the tower for measurement of the vertical heat, moisture, and momentum fluxes together with radiation fluxes. The depth is 2.5 m.

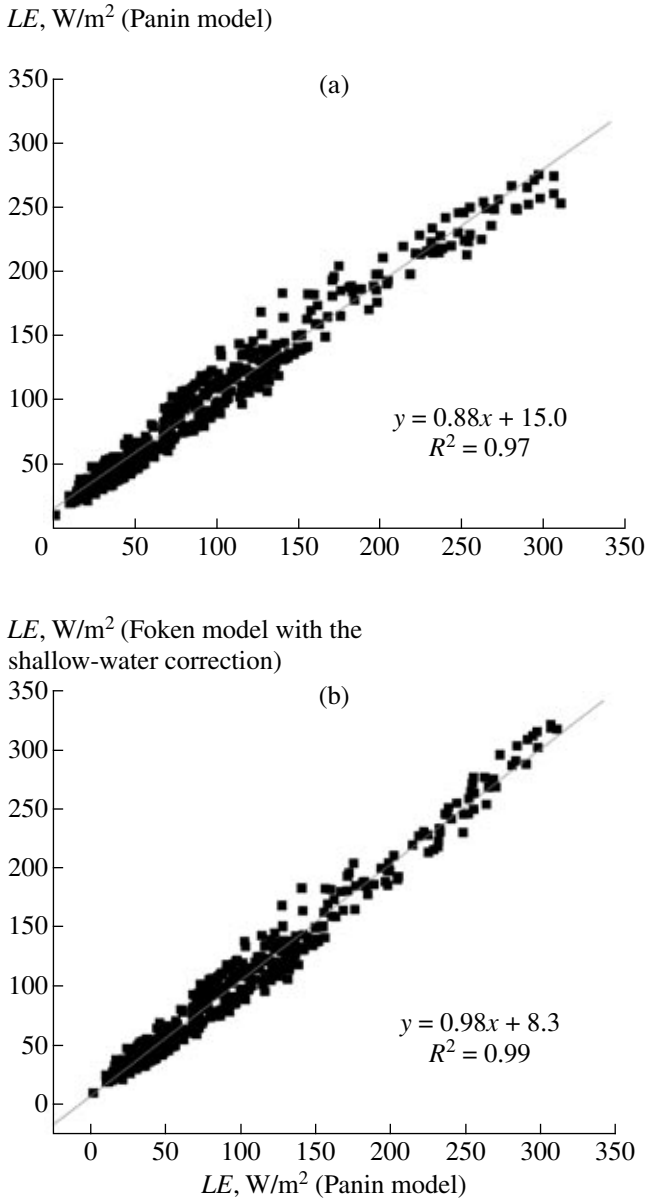

Fig. 6. Comparison of the latent heat exchange from the Panin model with the Foken model (a) without and (b) with a correction for the shallow-water effect at Great Kossenblatt Lake during the LITFASS-98 experiment.

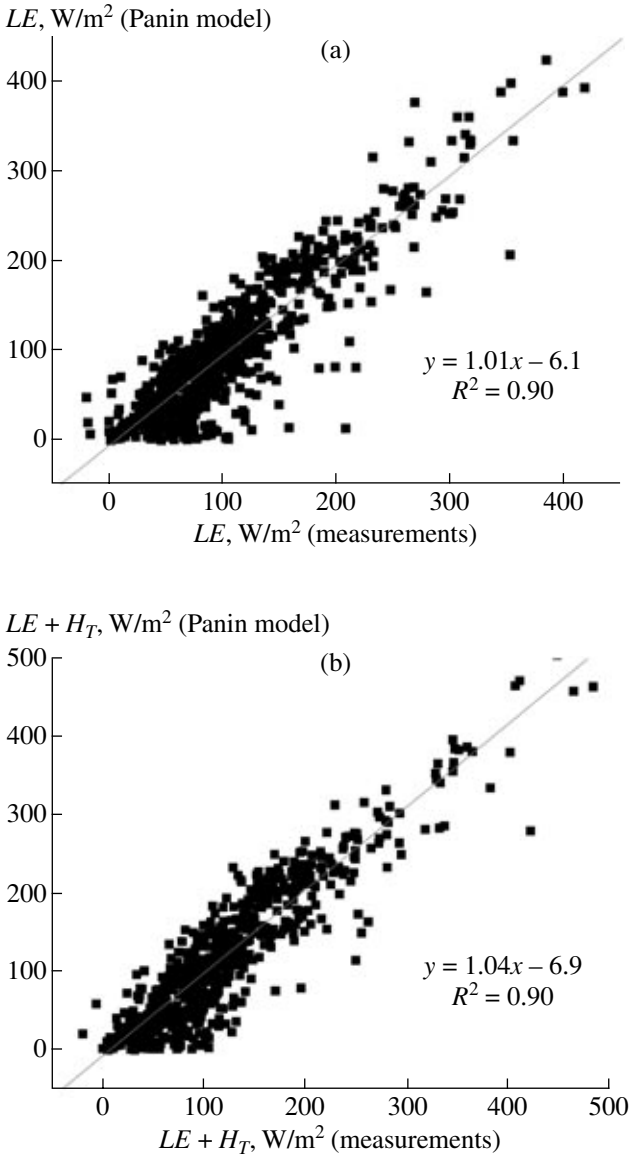

Fig. 7. Comparison of directly measured and calculated latent heat exchange (LE) and resultant heat exchange ($LE + H_T$) from the Panin model at Great Kossenblatt Lake during the LITFASS-2003 experiment for wind directions from 180° to 330°.

account the effect of the basin depth on water-surface friction.

There are a number of results from experimental studies where the coefficients a and b vary widely and show some dependence on the basin depth. Donelan's measurements [28] at Lake Ontario, at a depth of 10 m, gave values of 0.37 and 0.137 for a and b, respectively. Later measurements [29] at Lake Washington, at a depth of 4 m, yielded 0.87 and 0.078 for a and b, respectively. Graf's measurements on Lake Geneva, at a depth of 3 m, found a and b to be 1.09 and 0.094, respectively. Wieringa [30], at Lake Flevo, at a depth of 3 m, obtained 2.21 and 0.020 for a and b, respectively. Using the published data, we have determined the water-surface drag coefficient C_D at a wind speed of 10 m/s and analyzed its dependence on depth (Fig. 8a). The data of 12 independent experiments show a clearly defined dependence of C_D on depth.

Note that similar empirical relations can also be derived for other wind speeds. At low wind speeds (below 5 m/s), however, the correlation between the

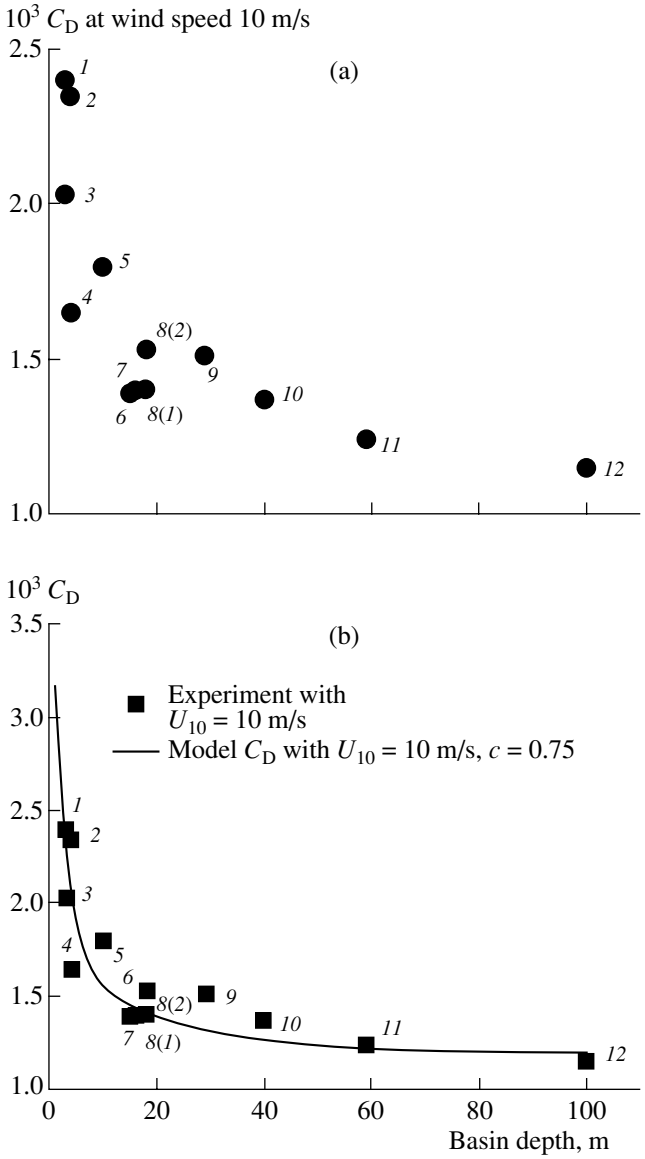

Fig. 8. (a) Drag coefficient (C_D) as a function of the depth of the sea at U_{10} = 10 m/s. Points *1–12* are experimental data: (*1*) Wieringa (1972), Lake Flevo (depth at the measurement point is 3 m); (*2*) Panin et al. (1996), Northern Caspian (depth at the measurement point 4 m; (*3*) Graf et al. (1984), Lake Geneva (depth at the measurement point 3 m); (*4*) Atakturk and Katsaros (1999), Lake Washington (depth at the measurement point 4 m); (*5*) Donelan (1982), Lake Ontario (depth at the measurement point 10 m); (*6*) Sheppard et al. (1972), Loch Ness (depth at the measurement point 15 m); (*7*) Geernaert et al. (1986), North Sea (depth at the measurement point 16 m); (*8*(*1*)) HERMAX experiment, North Sea (depth at the measurement point 18 m) (Smith et al., 1992); (*8*(*2*)) HERMAX experiment, North Sea (depth at the measurement point 18 m), momentum flux data reanalysis, Oost (1998); (*9*) Geernaert et al. (1987), North Sea (depth at the measurement point 29 m); (*10*) Kitaigorodskii et al. (1973), Caspian Sea (depth at the measurement point 40 m); (*11*) Smith; and (b) model calculation of the drag coefficient with c = 0.75 (straight line).

drag coefficient C_D and the basin depth decreases and the dependence becomes less distinct. Evidently, the role of boundary-layer stratification increases with decreasing wind speed. As a result, the dependence itself deteriorates.

A full overview of measurements of turbulent fluxes during light winds and their analysis was made by Kanta and Clayson [32]. Analysis of the energy and mass exchange between the deep sea and the atmosphere has shown that the wave age becomes an important parameter [31–35].

Here, particular attention is given to the interaction processes between the coastal shallow zone of the sea and the atmosphere.

Figure 8b clearly demonstrates the nearly full coincidence of the drag coefficient C_D calculated from our model at c = 0.75 with the data of all 12 independent experiments.

5. ESTIMATION OF THE SHALLOW-WATER EFFECT FOR REFINEMENT OF EVAPORATION IN THE NORTHERN CASPIAN AND KARA-BOGAZ GOL

We now consider the new estimates of the role of the depth in evaporation from the northern Caspian, but first we present a brief analysis of the wind and wave regime of this region.

The largest impact on the intensification of evaporation in the northern Caspian, as was noted above, may come from a storm wind. The severest storm occurred there in November 1952. It was caused by a steady southeasterly wind of long duration (four days). The wind speed during the storm attained 34 m/s.

The frequency of wind speeds (without regard for direction) is presented in Tables 1 and 2 and indicates that strong winds (above 15 m/s) account for 3% of cases. At the same time, the number of days in a year with winds over 15 m/s, e.g., at Fort Shevchenko, may be as large as 40 to 70.

According to Skriptunov's data (Table 2), wind speeds do not exceed 5 m/s in 55% of cases. This means that it is important to take into account the shallow-water effect in 45% of cases. As the wind speed increases, the duration of its action decreases (Table 3).

In the northern Caspian, waves can reach the maximum development possible in shallow basins, with breaking of all high and medium waves, a result that may cause a considerable intensification of the evaporation and heat exchange in this region. Because the Northern Caspian has shallow depths, the waves rapidly become steady when the wind arises. Wave parameters have a weak dependence on wind direction. The waves are characterized by a high steepness, which in a fully developed sea may reach a limiting value of 1/7.

With respect to wave-regime features and wave-growth conditions, the northern Caspian can be divided into two areas eastern and western. The eastern area is very shallow, with maximum depths of 8 m in its central part (Ural trough). The western area resembles an open bay on the side of the middle Caspian, with a shallow estuarine zone of the Volga River in the northern part.

In the northern Caspian, the frequency of waves is closely related to the frequency of winds. Easterly winds prevail throughout the year, especially in winter months. Their frequency is about 30% in winter and 10% in June and July. The southeasterly wind is characterized by the same annual cycle of frequency. This is probably linked to the effect of the Siberian High, which reaches the maximum development in winter and nearly disappears in summer. Westerly, northwesterly, and northerly winds have a higher frequency of occurrence in summer months (June and July). The frequency of northeasterly winds varies within narrow limits throughout the year except for December, when it is minimal (8.4%). Southerly and southwesterly winds occur rarely. Calms are most frequent in the summer months and in the early fall (July, August, September, and October).

The intensification of evaporation and heat exchange in this region may also be caused by storm surges. The vast shallows of the northern Caspian, small bottom and dry-land slopes, configuration of the shoreline, and intense wind activity are favorable for the development of considerable storm surges.

As follows from Fig. 3a, it can be noted that evaporation from shallows in natural conditions (at typical wind speeds) may be 1.5–2 times the value of evaporation from a deep sea. Actually, the frequency of strong winds (over 15 m/s) is low (Tables 1–3) and, therefore, their contribution to the total evaporation should not be so large.

We now turn to the corresponding estimates for the northern Caspian. In accordance with our model, to estimate the shallow-water effect, it is necessary to have statistical information about wind speed and frequency and information about depths and areas. Separately from the Kara-Bogaz Gol, consider the bathymetric chart of the Caspian Sea (Fig. 9) compiled from the bathymetric data of Lavrov (Fig. 10).

Examples of the calculation of evaporation intensification for the northern Caspian are given in Figs. 11a and 11b for winds of 10 and 20 m/s, respectively.

Our estimates show that evaporation in the coastal northern Caspian increases by 15% at wind speeds of 10 m/s and by 30% at 20 m/s. In the deeper middle part of the northern Caspian, the evaporation intensification due to consideration for the sea depth is 5 and 10%, respectively.

Table 1. Frequency of wind speeds by gradations (Aliev et al., 1988)

Wind speed, m/s	Frequency, %	Wind speed, m/s	Frequency, %
Below 2	6	10–12	12
2–4	14	12–14	7
4–6	20	14–16	3
6–8	19	16–18	2
8–10	16	Above 18	1

Table 2. Frequency (%) of wind speeds at Tyulenii Island in April–November 1937–1995 (from Skriptunov)

Wind speed, m/s	Frequency, %
Calm	13.07
1–5	42.4
6–10	37.3
11–15	5.9
16–20	1.25
21–25 or more	0.08

Table 3. Frequency (%) of wind speeds by gradations and duration at Fort Shevchenko (Koshinskii, 1975)

Wind speed, m/s	Lower limit of duration, h			
	6	12	24	48
Below 3	25	20	8	1
4–6	24	12	3	0.2
7–9	23	10	2	–
10–14	26	14	8	0.4
15–19	28	8	2	–
20–24	33	12	–	–

The interannual variation of the evaporation E from the surface of the northern Caspian differs greatly from that obtained earlier [3]. The annual mean evaporation from the northern Caspian made up 114.9 cm, or 14 cm higher than that calculated in our model without considering shallows [3].

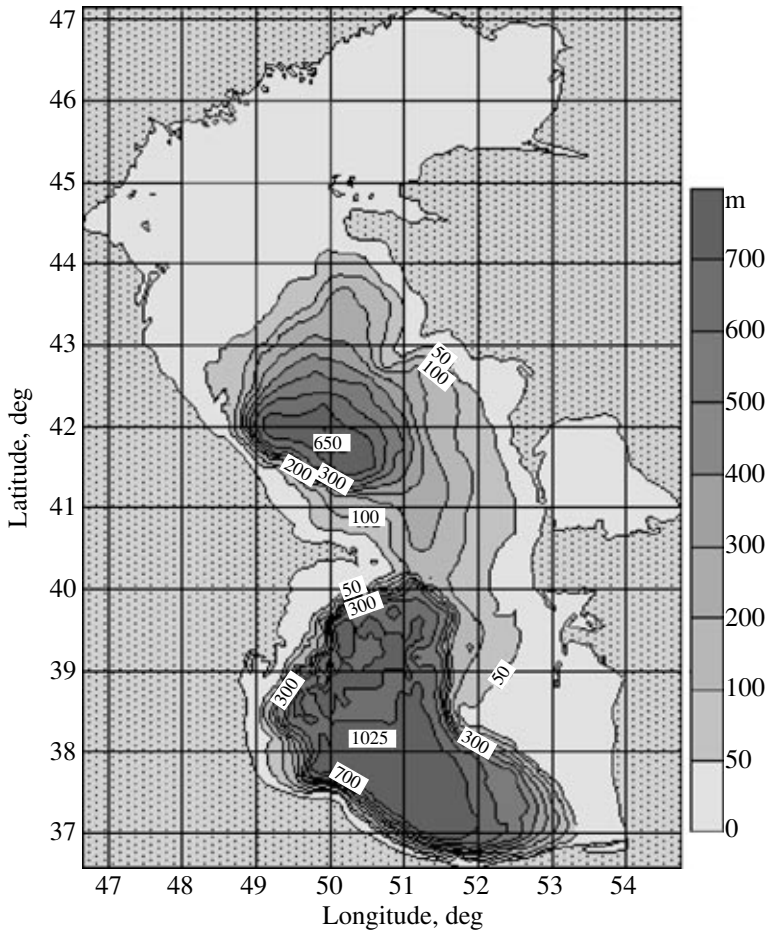

Fig. 9. Bathymetric chart of the Caspian Sea.

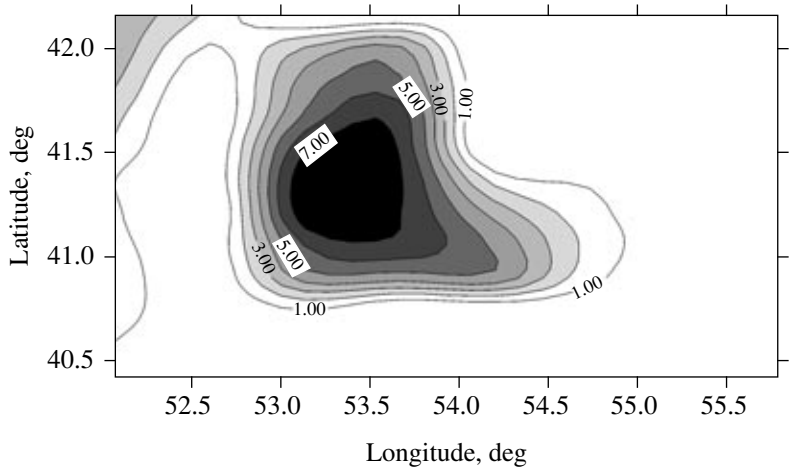

Fig. 10. Bathymetric chart of the Kara-Bogaz Gol in summer 1999 (from Lavrov's data).

As an example, distributions of the long-term means (for the period from 1904 to 1987) of latent heat over the Caspian Sea area in April (Figs. 12a, 12b) and July (Figs. 13a, 13b) are given without and with consideration for the intensification of vertical exchange with depth.

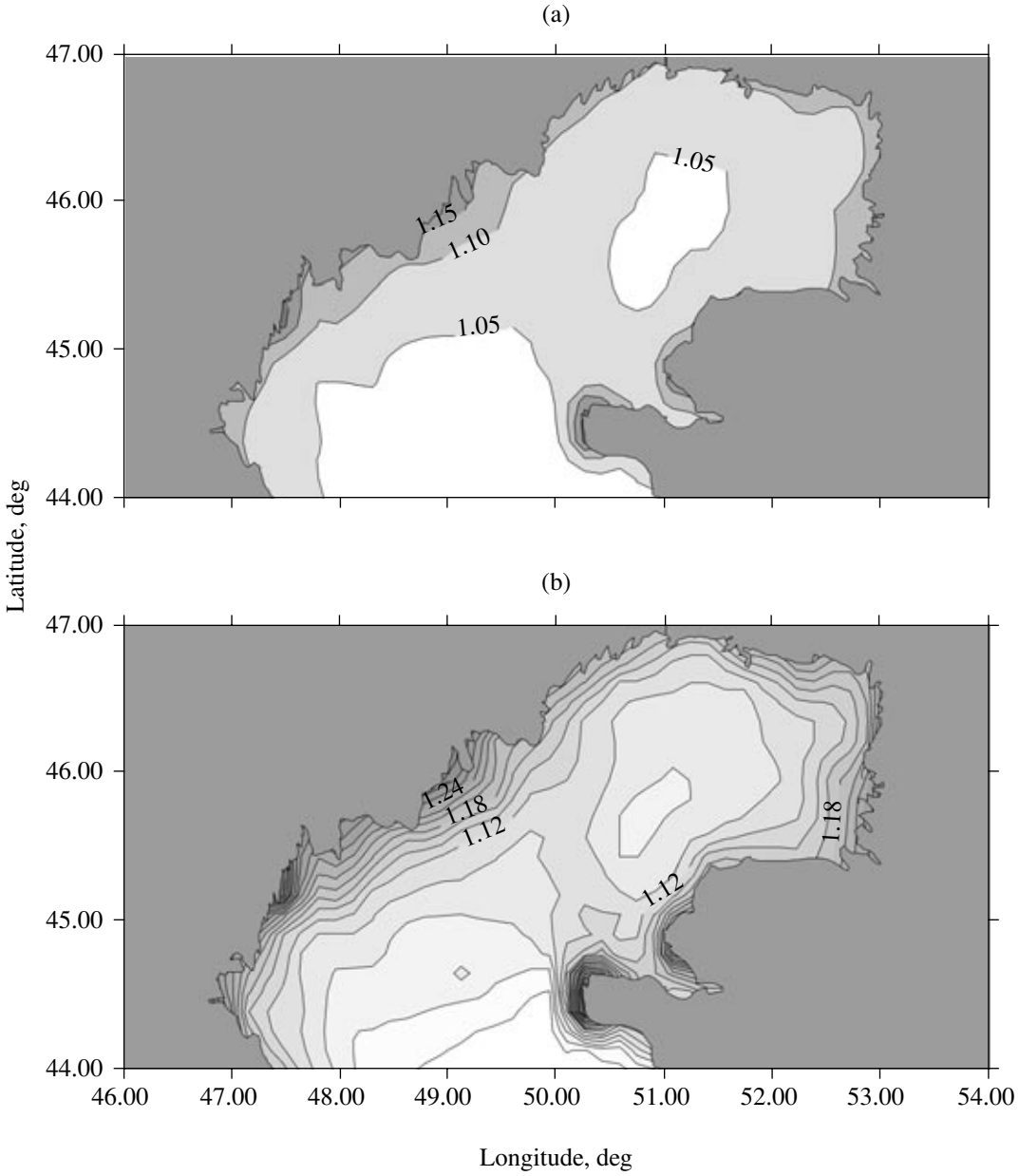

Fig. 11. Results from model calculation of evaporation intensification in the northern Caspian at (a) 10 m/s and (b) 20 m/s.

Thus, it may be concluded that the proposed model of the heat and moisture exchange of shallow and coastal water areas with the atmosphere allows refinement of the characteristics of the air–sea interaction on the basis of standard hydrometeorologic information. To design and test the model, not only direct measurements of turbulent momentum, heat, and moisture fluxes but also surface-wave characteristics were used. Data were obtained in deep and shallow areas of the open sea and in its coastal zones. The new model makes it possible to estimate the direct influence of the depth of a basin on the energy and mass exchange, both in the open sea and in the coastal zones.

On the one hand, the examples given here are indicative of a significant influence of the basin depth on the intensity of energy exchange in natural conditions. On the other hand, the examples illustrate that the model results are in good agreement with experimental data. Under real conditions, with the use of direct measurements of the area, depth, and wind frequency, the correction for the shallow-water effect

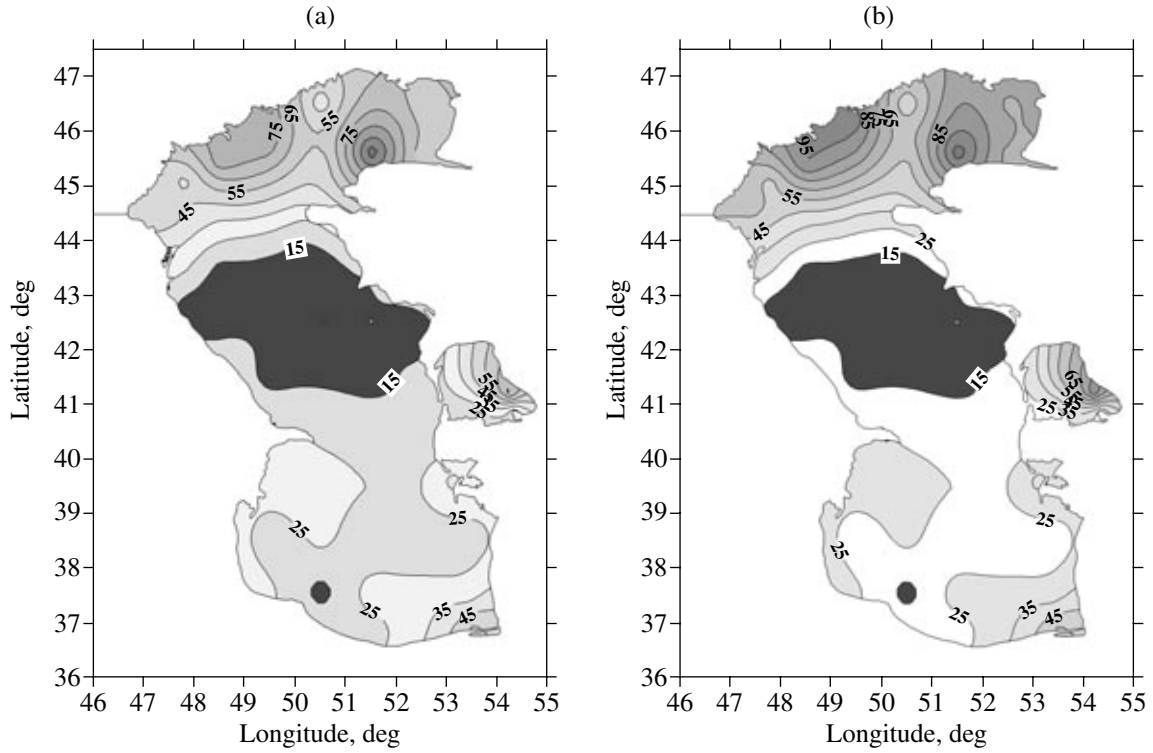

Fig. 12. Distribution of the long-term means (from 1904 to 1987) of latent heat across the Caspian Sea in April (a) without and (b) with the correction for vertical exchange intensification due to depth.

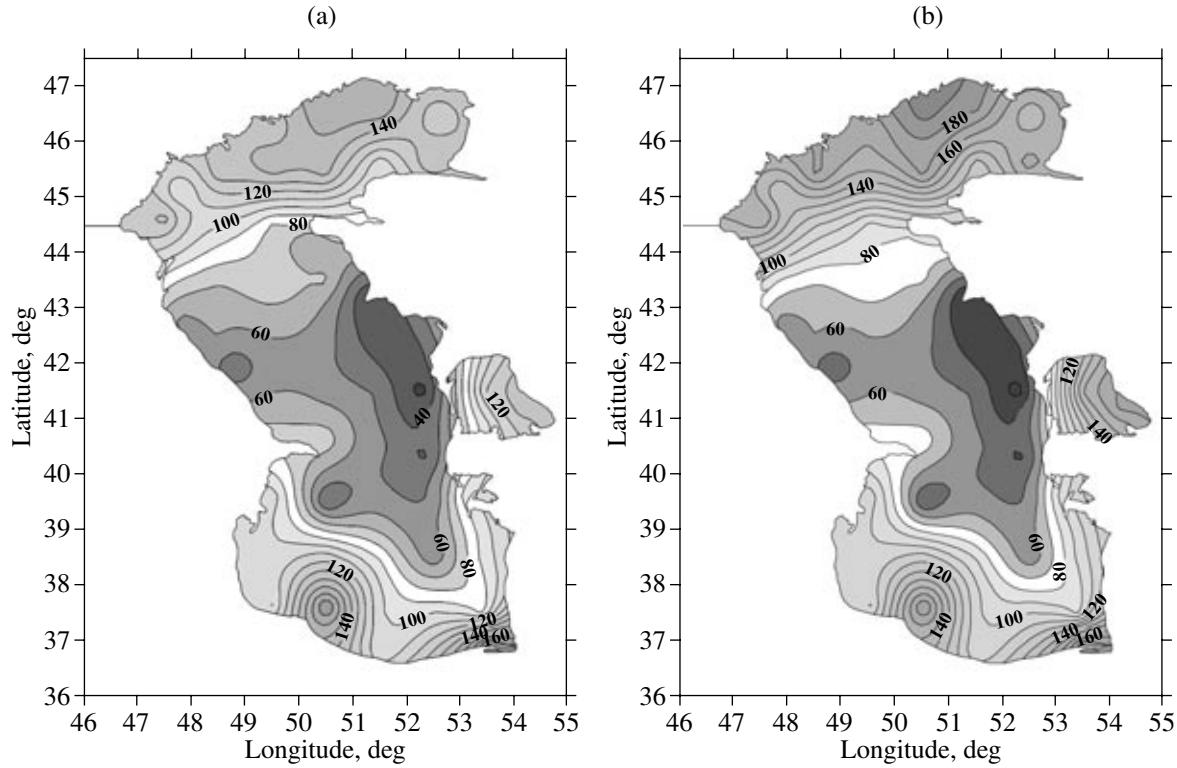

Fig. 13. Distribition of the long-term means (from 1904 to 1987) of latent heat across the Caspian Sea in July (a) without and (b) with the correction for vertical exchange intensification due to depth.

gives a 14% increase in the resultant evaporation from the northern Caspian.

CONCLUSIONS

It may be stated that the results obtained point to a substantial omission in investigating the nature of the water body–atmosphere interaction. The overview of the methods of calculation of evaporation and heat and energy exchange has shown that the up-to-date models of heat and mass exchange between a body of water and the atmosphere do not take into account the features of the small-scale interaction between shallows and the atmosphere. Waves in shallow zones are steeper than in the open and deep sea and break earlier (at lower wind speeds). All this leads to an increase in the aerodynamic roughness of the water surface and, consequently, to a more intense turbulent exchange of momentum, heat, and moisture. The overview has also shown that there is still no reliable method of estimation of evaporation and heat exchange in shallow lakes and sea coastal zones.

It is shown that comparison of different parameterizations used for the calculation of sensible and latent heat fluxes in the open sea and corrected for the shallow-water effect provides good results. Even at low wind speeds, the effect of the flux increase in shallow lakes (by example of the LITFASS-98 and LITFASS-2003 experiments) attains a value of 10 to 20%, larger than the differences between the calculated and measured fluxes. This means that the proposed parameterization is well suited for the lakes where a standard dataset is available on wind speed, air and water temperature, air humidity, and depth. The model of the energy exchange between a body of water and the atmosphere in the coastal zone also agrees well with experimental data on the drag coefficient measured by various investigators.

Overall, our theoretical generalizations and experimental investigation of the role of the basin depth in the intensification of evaporation, heat exchange, and water-surface friction and first estimates of the role of this factor in the evaporation from the northern Caspian strongly suggest that the new model is universal. On the one hand, the results are indicative of a significant influence of the basin depth on the intensity of energy exchange under natural conditions. On the other hand, the examples presented illustrate good agreement of the model calculations with experimental data. Under real conditions, with the use of direct data on the depth, area, and wind frequency, the correction for the shallow-water effect gives an increase in the resultant evaporation from the northern Caspian above 10%.

The features of the spatial variability of the Caspian Sea evaporation also suggest that there may be an external forcing of the formation of surface currents, which was disregarded earlier in the simulation of currents. This forcing is caused by heterogeneous evaporation (intense evaporation in spring and in the first half of summer in the northern and southern parts of the Caspian leads to a level difference between the middle Caspian and these parts) and may exert significant influence on the water circulation in the entire sea. It might be expected that this circulation, which is intensified in spring and in the first half of summer because of the intense evaporation from the shallow northern Caspian, is seasonal in character. In the fall and early winter, the evaporation field becomes homogeneous in space, and quite a different picture in the field of currents might be expected. Evidently, similar currents can be simulated within the framework of a three-dimensional thermohydrodynamic model (for example, the hydrodynamic inland sea model (HISM)). The HISM is a coupled model of three-dimensional thermohydrodynamic processes of the sea, the model of the interaction between the boundary layers of the atmosphere and the sea, and the sea-ice thermohydrodynamic model. A fundamentally important feature of the HISM is its ability to reproduce processes related to water exchange across the side boundaries (river runoff, exchange through straits); the variability of the water mass in the sea and, consequently, of the upper boundary of the sea; sea-surface topography variability, which results from the response of the sea to rapid changes in external forcing; air–sea interaction; and formation of sea ice and its influence on the heat and moisture exchange between the atmosphere and the sea [36]. The first numerical experiments provide encouraging results. The model reproduces the seasonal variability of monthly mean currents on the sea surface, a phenomenon that can be divided into three periods: prevailing cyclonic gyres in the middle and southern Caspian, typically observed in December–January; dominant Ekman transport of surface waters to the south and southwest in the deep parts of the middle and southern Caspian from February through August; and transitional currents between the two indicated types from September through November. An important argument in support of the existence of the surface cyclonic flow system is the spread of warm waters northward along the eastern coast of the sea. Results of the model experiments show that the northward current along the eastern coast exists stably, but only in the subsurface layer, whereas the surface currents are often directed southward. Analysis of observations of currents confirms the structure of currents on the eastern shelf that was simulated by the model.

ACKNOWLEDGMENTS

This study was supported by the Program for Basic Research of the Earth Science Division of the Russian Academy of Sciences no. 11 “Hydrospheric and Atmospheric Processes: Formation, Change, and Control of the Earth’s Climate.”

REFERENCES

1. A. S. Monin and A. M. Yaglom, *Statistical Fluid Mechanics* (MIT Press, Cambridge, 1971; Gidrometeoizdat, St. Petersburg, 1992).
2. G. N. Panin, *Heat and Mass Exchange between a Body of Water and the Atmosphere in Natural Conditions* (Nauka, Moscow, 1985) [in Russian].
3. G. N. Panin, *Evaporation and Heat Exchange for the Caspian Sea* (Nauka, Moscow, 1987) [in Russian].
4. G. S. Golitsyn and G. N. Panin, "On the Water Balance and the Current Variations in Caspian Sea Level," Meteorol. Gidrol., No. 1, 57–64 (1989).
5. G. N. Panin and A. E. Nasonov, "Problems of Measurement and Calculation of Surface Fluxes in KUREX-91 Experiment," Remote Sensing Rev. **17**, 281–290 (1998).
6. E. T. Kanemasu, S. B. Verma, E. A. Smith, et al., "Surface Flux Measurements in FIFE: An Overview," J. Geophys. Res. D **97**, 18547–18556 (1992).
7. T. Foken, "The Parametrisation of the Energy Exchange across the Air–Sea Interface," Dyn. Atmos. Oceans **8**, 297–305 (1984).
8. T. Foken, "An Operational Model of the Energy Exchange across the Air–Sea Interface," Z. Meteorol. **36**, 354–359 (1986).
9. T. Foken, S. A. Kitajgorodskij, and O. A. Kuznecov, "On the Dynamics of the Molecular Temperature Boundary Layer above the Sea," Boundary Layer Meteorol. **15**, 289–300 (1978).
10. G. N. Panin and S. V. Krivitskii, *Aerodynamic Roughness of the Surface of a Water Body* (Nauka, Moscow, 1992) [in Russian].
11. S. A. Kitaigorodskii, O. A. Kuznetsov, and G. N. Panin, "On the Coefficients of Resistance, Heat Transfer, and Evaporation in Calculations of Momentum, Heat, and Moisture Fluxes over the Sea Surface in the Atmosphere," Izv. Akad. Nauk SSSR, Fiz. Atmos. Okeana. **9**, 1135–1141 (1973).
12. G. N. Panin, A. Raabe, S. V. Krivitskii, et al., "Small-Scale Air–Sea Interaction in the Coastal Zone," Vodn. Resur. **21**, 59–68 (1994).
13. A. Yu. Benilov, O. A. Kuznetsov, and G. N. Panin, "On the Analysis of Wind Wave-Induced Disturbances of the Atmospheric Turbulent Surface Layer," Boundary-Layer Meteorol. **6**, 269–285 (1974).
14. G. N. Panin, "Some Experimental Results from Studies of Air–Sea Interaction," Boundary-Layer Meteorol. **50**, 147–152 (1990).
15. G. S. Golitsyn and A. A. Grachev, "Velocities and Heat and Mass Exchange during Convection in a Two-Component Medium," Dokl. Akad. Nauk SSSR **255**, 548–552 (1989).
16. A. Raabe, G. N. Panin, and H.-Y. Schoenfeldt, "Die Variabilitat des Windreibungs-Koeffizienten Uber See in der Nahe Einer Kuste Mit Steil Ansteigendem," Ufer. Z. Meteorol. **37** (3), 137–147 (1987).
17. G. N. Panin, A. E. Nasonov, and M. G. Souchintsev, "Measurements and Estimation of Energy and Mass Exchange over a Shallow Sea," in *The Air–Sea Interface*, Ed. by M. Donelan (Rosenstiel School of Marine and Atmospheric Sciences, Miami, Florida, 1996), pp. 489–494.
18. A. F. G. Jacobs, B. G. Heusinkveld, and J. P. Nieveen, "Temperature Behavior of a Natural Shallow Water Body During a Summer Periode," Theor. Appl. Climatol. **59**, 121–127 (1998).
19. V. I. Naidenov, *Nonlinear Dynamics of Surface Waters of Dry Land* (Nauka, Moscow, 2004) [in Russian].
20. G. N. Panin, A. E. Nasonov, Th. Foken, and H. Lohse, "Evaporation and Sensible Heat Exchange for a Shallow Lake," Theor. Appl. Climatol. **28** (2006) (in press).
21. R. B. Stull, *An Introduction to Boundary Layer Meteorology* (Kluwer, Dordrecht, 1988).
22. I. N. Davidan, L. I. Lopatukhin, and V. A. Rozhkov, *Waves in the Ocean* (Gidrometeoizdat, Leningrad, 1985) [in Russian].
23. M. Boorngen, H.-J. Schoenfeldt, F. Riechmann, et al., *Wind Atlas and Wave Atlas for the Area of Darss and Zingst* (Wiss. Mitteilungen Inst. fur Meteorology, Leipzig, 1998), Vol. 10.
24. WADIM Group (S. Hasselman, K. Hasselman, P. A. E. M. Janson, et al.), "The WAM Model—A Third Generation Ocean Wave Prediction Model," J. Phys. Oceanogr. **18**, 1775–1810 (1988).
25. F. Beyrich, *LITFASS-98 Experiment, 25.5.1998–30.6.1998, Experimental Report* (Deutscher Wetterdienst, Forschung und Entwicklung, Arbeitsergebnisse, Frankfurt am Main, 2000), No. 62.
26. F. Beyrich, H.-J. Herzog, and J. Neisser, "The LITFASS Project of DWD and the LITFASS-98 Experiment: The Project Strategy and the Experimental Setup," Theor. Appl. Climatol. **73** (3/4), 3–18 (2002).
27. G. L. Geernaert, "Bulk Parametrizations for the Wind Stress and Heat Fluxes," in *Plant Surface Waves and Fluxes*, Ed. by G. L. Geernaert and W. J. Plant (Dordrecht, Kluwer, 1990), Vol. 1, pp. 91–172.
28. M. A. Donelan, "The Dependence of the Aerodynamic Drag Coefficient on Wave Parameters," in *Proceedings of First International Conference on Meteorology and Air–Sea Interaction of the Coastal Zone* (American Meteorological Society, 1982), pp. 381–387.
29. S. S. Atakturk and K. B. Katsaros, "Wind Stress and Surface Waves Observed on Lake Washington," J. Phys. Oceanogr. **29**, 633–650 (1999).
30. J. Wieringa, "Tilt Errors and Precipitation Effects in Trivane Measurements of Turbulent Fluxes over Open Water," Boundary-Layer Meteorol. **2**, 406–426 (1972).
31. J. R. Garratt, "The Internal Boundary Layer—A Review," Boundary-Layer Meteorol. **50**, 171–203 (1990).
32. L. H. Kanta and C. A. Clayson, *Small Scale Processes in Geophysical Fluid Flows* (Academic, 2000).
33. V. N. Kudryavtsev, V. K. Makin, and J. F. Meirink, "Simplified Model of the Air Flow above Waves," Boundary-Layer Meteorol. **100**, 63–90 (2001).
34. W. A. Oost, "The KNMI HEXMAX Stress Data—A Reanalysis," Boundary-Layer Meteorol. **86**, 447–468 (1998).
35. H. P. Schmid, "Experimental Design for Flux Measurements: Matching Scales of Observations and Fluxes," Agric. For. Meteorol. **87**, 179–200 (1997).
36. R. A. Ibraev, "Sensitivity of the Solution of a Model for the Dynamics of Black Sea Currents to the Condition of the Free Sea Surface," Okeanologiya **41**, 645–652 (2001).

Translated by N. Tret'yakova